

Clinical indications for digital imaging in dento-alveolar trauma. Part 1: traumatic injuries

Cohenca N, Simon JH, Roges R, Morag Y, Malfaz JM. Clinical indications for digital imaging in dento-alveolar trauma. Part 1: traumatic injuries. © Blackwell Munksgaard, 2006.

Abstract – Traumatized teeth present a clinical challenge with regard to their diagnosis, treatment plan, and prognosis. Recent developments in imaging systems have enabled clinicians to visualize structural changes effectively. Computed tomography, magnetic resonance imaging and cone beam computed tomography are among the most commonly used systems for dental and maxillofacial surgery. The purpose of this review is to describe the advantages and disadvantages of each technique and the clinical application for dento-alveolar trauma. Three clinical cases are described to illustrate the potential use of the NewTom 3G for diagnosis and treatment plan of dento-alveolar traumatic injuries.

**Nestor Cohenca¹, James H. Simon²,
Ramon Roges², Yoav Morag³,
Jose Maria Malfaz²**

¹Department of Endodontics, School of Dentistry, University of Washington, Seattle, WA; ²Division of Surgical, Therapeutic and Bioengineering Sciences, University of Southern California School of Dentistry, Los Angeles, CA; ³Department of Radiology, University of Michigan, Ann Arbor, MI, USA

Key words: dental trauma; diagnosis; digital imaging; computed tomography; cone beam computed tomography; luxation injuries; root fracture

Nestor Cohenca, Department of Endodontics, University of Washington, POB 357448, Seattle, WA 98195-7448, USA

Tel.: +1 206 543 5044

Fax: +1 206 616 9085

e-mail: cohenca@u.washington.edu

Accepted 23 March, 2006

The past decade has witnessed several changes in the world of endodontics. New technologies, instruments and materials have resulted in a better diagnosis and more predictable endodontic therapy. Recent improvements in digital radiographic imaging have introduced a new dimension with many potential benefits for endodontic practice. Digital radiography (1), computed tomography (CT) (2–4), magnetic resonance imaging (MRI) (5) and more recently cone beam computed tomography (CBCT) (6–9) have become increasingly important in diagnosis and treatment planning.

The traditional projection (plain film) radiograph is a two-dimensional shadow of a three-dimensional (3-D) object. Three-dimensional imaging overcomes this major limitation by allowing us to visualize the third dimension while at the same time eliminating superimpositions. Previous studies reported the use of CT and digital radiography for differential diagnosis of periapical pathology (10, 11) and treatment outcomes (12, 13). The use of 3-D imaging systems in oral and maxillofacial surgery

has been extensively reported in the literature (3, 5, 14–16). However, the potential use of 3-D imaging for the diagnosis of dental trauma has not been reported.

The incidence of dental trauma as a result of falls, bicycle accidents, skateboarding and other sports activities is higher in children and adolescents, with the maxillary incisor teeth most commonly affected (17–19). The first clinical and radiographic examination of the traumatized patient is crucial to determine the initial diagnosis, severity of the injury, treatment plan and to create a baseline for follow up. Common diagnostic aids for pulpal and periapical conditions are percussion, palpation, tooth mobility, coronal color changes, pulp sensitivity tests, and radiographs. When correctly performed and adequately interpreted these tests are reliable in diagnosing pulp necrosis (20).

The purpose of this review is to discuss different techniques of 3-D imaging and to illustrate the clinical application of the CBCT for diagnosis and treatment plan of traumatic injuries.

Computed tomography

Computed tomography uses X-rays to portray a cross-sectional image of an object without superimpositions (21). The CT scanner makes multiple projections of an object with a thin beam of X-rays. Radiation detectors measure the object's X-ray attenuation at each of these projections and a computer reconstructs the attenuation data to produce a cross-sectional image of the object (22).

The first clinical CT X-ray unit was developed in 1972 by G.N. Hounsfield (23) in England and it revolutionized clinical imaging by offering three major advantages – no superimpositions, the ability to distinguish between objects of similar density (contrast resolution), and digitally acquired data, therefore offering greater flexibility in processing, analyzing, and storing of information. Improvement in contrast and temporal resolution of early CT scanning was achieved by the introduction of helical CT scanners and multi-detector computed tomography (MDCT) (24). The slip ring technology of helical CT scanners enabled continuous uninterrupted acquisition of volumetric data with reduced scan times. The multiple rows of detectors in MDCT expanded the speed of scanning, thus enabling breath hold imaging acquisition, resulting in improvement in 3-D reconstructed images in virtually any plane. Sixteen-detector row MDCT can acquire substantial anatomic volumes with isotropic sub-millimeter spatial resolution and scan times of <10 s for 300 mm of coverage (25).

Computed tomography imaging is extremely important in maxillofacial trauma and has become the gold standard in imaging for these cases (26). Other dental and maxillofacial indications for CT include the study of growth and development, oral pathology, salivary gland disease, and treatment plan and placement of dental implants. The main disadvantages of CT are the high radiation dose compared with plain-film radiography and the high cost of the equipment. Image acquisition time has decreased dramatically with the introduction of MDCT (24) but this has come at the expense of reduced radiation dose efficiency.

Magnetic resonance imaging

Magnetic resonance imaging is a modern computerized method of scanning and creating images using a strong magnetic field and radio waves. The hydrogen atoms in the patient's body react with the magnetic field and as a result of a radiofrequency pulse, emit their own radiofrequency signal which is analyzed by a computer to produce images. The images obtained help in detecting various abnormalities in the tissues scanned. MRI is based on the

principles of nuclear magnetic resonance (NMR), a spectroscopic technique used by scientists to obtain microscopic chemical and physical information about molecules (27). The technique was called MRI rather than nuclear magnetic resonance imaging (NMRI) because of the negative connotations associated with the word nuclear in the late 1970s. MRI started out as a tomographic imaging technique, in that it produced an image of the NMR signal in a thin slice through the human body.

Felix Bloch and Edward Purcell, both of whom were awarded the Nobel prize in 1952, discovered the magnetic resonance phenomenon independently in 1946. In 1975 Richard Ernst proposed MRI using phase and frequency encoding, and Fourier transformation. This technique is the basis of current MRI techniques. A few years later, in 1977, Raymond Damadian was the first to ever perform an MRI examination on a human being (28). In the same year, Peter Mansfield developed the echo-planar imaging (EPI) technique. This technique was developed in later years to produce images at video rates (30 ms/image) (29).

Although the spatial resolution of MRI is inferior to CT, the advent of the 3 Tesla MRI may provide improved spatial resolution in addition to the already superior contrast resolution of the MRI. High-resolution T2-weighted imaging of a finger provided a voxel size of $0.19 \times 0.19 \times 0.42$ mm (30).

Imaging and analysis using magnetic resonance brings exciting possibilities to medical and dental specialties without concerns about radiation dose. However, MRI is less sensitive for osseous injury and its application in the oro-facial field include diagnosis of tumors of the oral cavity, pharynx, larynx, paranasal sinuses, as well as diagnosis for temporomandibular joint and salivary gland diseases (31). The main disadvantage of MRI falls into the cost of the equipment and its interpretation.

Cone beam computed tomography

Cone beam computed tomography, also called digital volume tomography (DVT), is a new technique that produces 3-D digital imaging at reduced cost and less radiation for the patient than traditional CT scans (14). It also delivers a faster and easier image acquisition.

The NewTom 3G DVT 9000 (Quantitative Radiology s.r.l., Verona, Italy) was the first CBCT introduced to the United States' market in 2001. Since then, several other systems have been commercialized, including CB MercuRay (Hitachi Medical Corp., Chiba-ken, Japan), 3D Accuitomo-XYZ Slice View Tomograph (J. Morita Manufacturing, Kyoto, Japan), and iCat (Xoran Technologies, Ann

Arbor, MI, USA/Imaging Sciences International, Hatfield, PA, USA).

The NewTom 3G acquires 360 images at 1° intervals in 36 s, with reconstructed image resolution of 512 × 512 pixels and 12 bits per pixel (4096 grayscale). The pixel size varies between 0.25 and 0.42 mm depending on the user's choices (large or small field and the sensor, 9 or 12 in). The axial slice thickness can be set up between 0.1 and 5 mm.

Dental applications of CBCT imaging have been reported for oral and maxillofacial surgery (14, 32, 33), implantology (34, 35), and orthodontics (7, 36, 37). Studies have suggested that CBCT provides accurate and reliable linear measurements for reconstruction and imaging of dental and maxillofacial structures (8, 38, 39).

Comparison between CBCT, CT, and MRI

Cone beam computed tomography results in a fraction of the effective absorbed dose of radiation (*E*) compared with a traditional CT scan. Imaging of a maxillomandibular volume with the NewTom 3G results in an *E* of 57 µSv (6) while traditional medical CTs result in an *E* of 1400 µSv for a maxillary CT scan and 2100 µSv for a maxillomandibular examination (40). For purposes of comparison a panoramic radiograph results in an *E* of 6 µSv and a full mouth series results in an *E* from 33 to 84 µSv (41) and 14 to 100 µSv (42) depending upon variables such as film speed, technique, kVp, and collimation.

Hashimoto et al. (43) reported that CBCT (3DX multi-image micro-CT) is more efficient than MDCT for diagnosis and examination of hard tissues in the maxillofacial region. Image quality of the CBCT was deemed superior to MDCT for evaluation of right central incisor and left mandibular first molar cortical and cancellous bone, enamel, dentin, pulp cavity, and periodontal ligament space lamina dura in an anthropomorphic phantom. In addition, the mean skin doses per examination with the MDCT were 458 mSv examinations vs 1.19 mSv with the CBCT. Mah et al. (44) compared the tissue-absorbed dose of CBCT and other computed tomographic imaging modalities. They concluded that the effective dose for imaging of maxillomandibular volume with a NewTom 9000 is significantly lower than that achieved with CT imaging methods. A comparative table evaluating technical characteristics and specifications of different CBCT devices, MDCT, and MRI is presented (Table 1) (7).

Magnetic resonance imaging has been infrequently used for dental evaluation despite the fact that it has the ability to demonstrate the neurovascular bundle within the mandibular canal, its relation to the teeth and reveal the pulp chambers of the

Table 1. Comparison of different CBCT devices, MDCT, and MRI

Parameters	NewTom 9000	3DX Accutomo	ISI/CAT	Hitachi MercuRay	Multi-DetectorCT	MRI Philips Achieva 3.0T
X-ray beam	Cone	Cone	Cone	Cone	Fan	NA
Sensor detector	Area image intensifier CCD	Area image intensifier CCD	Area amorphous silicon flat-panel detector	Area image intensifier CCD	Linear solid state or gas	Radiofrequency antennae
Grayscale	12 bit	8 bit	12 bit	8 bit	12 bit	12 bit
Voxel size (mm ³)	0.25–0.42	0.125	0.4	0.1	0.316	0.7 × 0.8 × 2.0 mm [†]
X-ray source	Fixed	Direct current	Direct current	Fixed	Rotating	NA
Anode	110 (fixed)	Fixed	Fixed	70–100	110–140	NA
kVp range	10–15 max	60–80	120	To 15 max	80–300	NA
mA	10–15 max	1–10	1–3	Panoramic type single 360° rotations	Axial slice multiple 360° rotations	NA
Image acquisition	Panoramic type single 360° rotations	Panoramic type single 360° rotations	Panoramic type single 360° rotations	Panoramic type single 360° rotations	Supine	Multisequence multiplanar image acquisition
Patient position	Supine	Seated	Seated	Seated	Supine	Supine
Image area	Maxillofacial	Maxillofacial	Maxillofacial	Maxillofacial	Entire body	Entire body
Imaging session (s)	75	17	40 or less	9.6	Varies/examination	Varies/examination
Effective dose* (max & mand) mSv	0.04–0.0515	0.0074	Not available	Not available	2.6–3.1	NA
Auto exposure control	Smart scan	No	Not reported	Not reported	No	NA
	Yes					

CBCT, cone beam computed tomography; MDCT, multi-detector computed tomography; MRI, magnetic resonance imaging; NA, not applicable.

*Effective dose as reported is provided from the manufacturer and is not truly comparable to other devices due to variable such as different size of imaging volumes and operational settings of the devices.

[†]Variable voxel size numbers quoted are used in 2-D multislice imaging.

teeth. MRI was found to be somewhat superior to CT in imaging the mandibular canal prior to dental implants (45) and comparable to CT in evaluation of jaw bone length measurements (46). Gahleitner et al. (47) reported that patients with inflamed dental pulp demonstrate bone marrow edema in the periapical region which would not be apparent on CT or CBCT.

Case 1

A 15-year-old male patient presented to the Endodontic Graduate Clinic at the University of Southern California with a complaint of discomfort on his front upper teeth. His medical history was noncontributory. A review of the dental history revealed an impact injury to the face due to a fall that occurred approximately 4 months prior. The patient was initially treated by his general dentist who diagnosed a root fracture on the maxillary left central incisor and applied a rigid splint with wire and composite resins extending from the maxillary left canine to the maxillary right canine (Fig. 1a).

Four months later, the patient was referred for endodontic consultation. Visual examination revealed bacterial plaque retention due to the splint and poor oral hygiene. Upon clinical examination, the maxillary left central incisor did not respond to an electric pulp sensitivity test (Vitality Scanner; Analytic Technologies, Redmond, WA, USA) or to a cold sensitivity test at -50°C (Endo Frost; Roeko, Langenau, Germany). The tooth was mobile but without sensitivity to percussion or palpation. The adjacent teeth were asymptomatic and responded

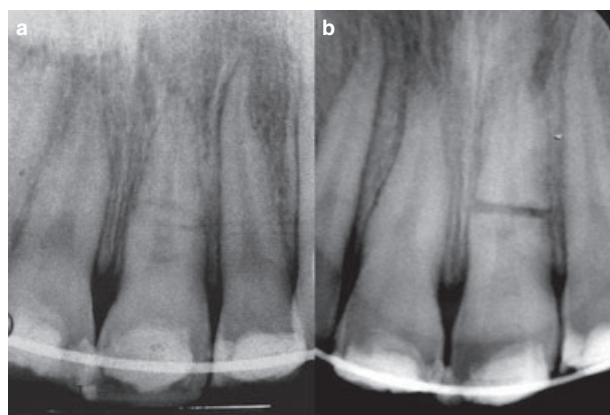


Fig. 1. (a) Periapical radiograph of the maxillary left central incisor following the initial diagnosis of a root fracture and application of a rigid splint using wire and composite resins extending from the maxillary left canine to the maxillary right canine. Close reduction in the fragments is evident. (b) Four months later, the radiograph shows a mid-root horizontal fracture with separation of the fragments and a radiolucent area at the fracture line. No apical pathology is observed.

normally to cold and electric pulp tests. Radiographic examination showed a mid-root horizontal fracture on the maxillary left central incisor with separation of the fragments and a radiolucent area at the fracture line (Fig. 1b). No apical pathology could be observed. The NewTom 3G DVT 9000 analysis at 0.2 mm cuts showed the horizontal root fracture from a cross-sectional view and demonstrated the oblique component of the fracture in the palatal aspect of the root (Fig. 2). Fracture of the alveolar bone at the level of the root fracture was also observed (Fig. 2c).

An initial diagnosis of pulp necrosis in the maxillary left central incisor was made and the patient was scheduled for endodontic therapy of the coronal fragment only. The treatment was uneventful and root canal filling was performed using white mineral trioxide aggregate (Pro Root, Dentsply; Tulsa Dental, Johnson City, TN, USA) (Fig. 3).

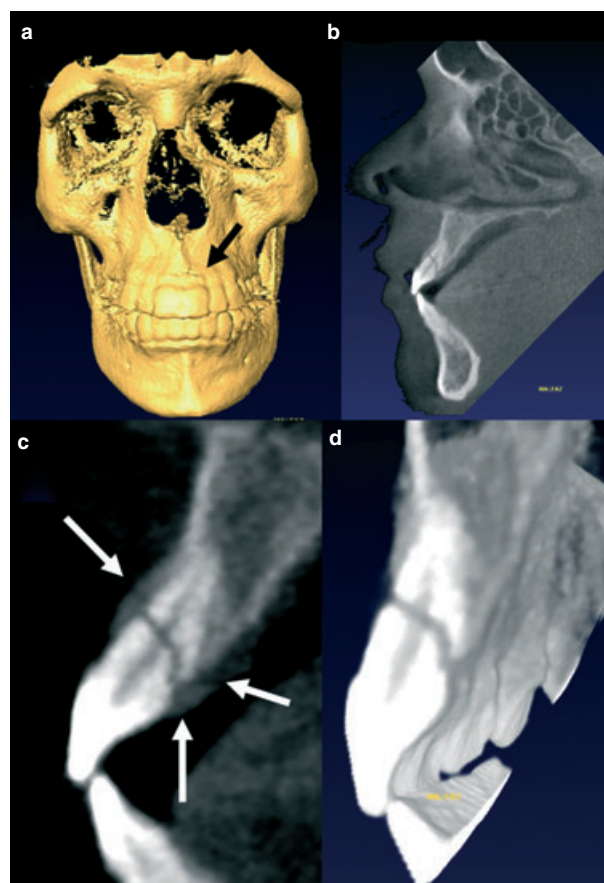


Fig. 2. (a) Frontal reconstruction with the NewTom demonstrating an alveolar fracture of the buccal plate at the level of the root fracture (see arrow). (b) Cross-sectional view confirms the mid-root horizontal fracture. (c, d) At closer view, 0.2 mm cuts show the horizontal root fracture with an oblique component in the palatal aspect of the root and the fracture of the alveolar bone in both buccal and palatal plates (see arrows).



Fig. 3. Immediate postoperative periapical radiograph showing the final obturation of the coronal fragment with mineral trioxide aggregate.

The patient was re-examined 10 months later. The maxillary left central incisor was asymptomatic and non-mobile. Follow-up radiographic examination was performed using plain periapical radiographs and the NewTom 3G DVT 9000. Periapical radiographs showed evidence of root remodeling and a significant reduction of the fragments without interposition of granulation tissue (Fig. 4a,b). Cross-sectional view with the NewTom revealed only a slight reduction in the space between the fragments with interposition of bone and connective tissue (Fig. 4c,d). Lack of healing in the palatal surface of the root may have been due to a double fracture of the root which can be seen in this cross-sectional proximal view (see arrow in Fig. 4d).

Case 2

A 24-year-old male patient presented to the Center for Urgent Care, Trauma and Sports Dentistry at the University of Southern California with severe trauma to his maxillary left central and lateral incisors after he fell down the stairs. His medical history was unremarkable.

Visual examination revealed a severe lateral luxation of both maxillary left incisors (Fig. 5a–c). Soft tissue lacerations and localized swelling of the lower and upper lips was also noted (Fig. 5c,d). The occlusion was altered and the patient was not able to bite in centric relation. Upon palpation of the buccal cortical plate, an alveolar fracture was suspected. Radiographically, periradicular radio-

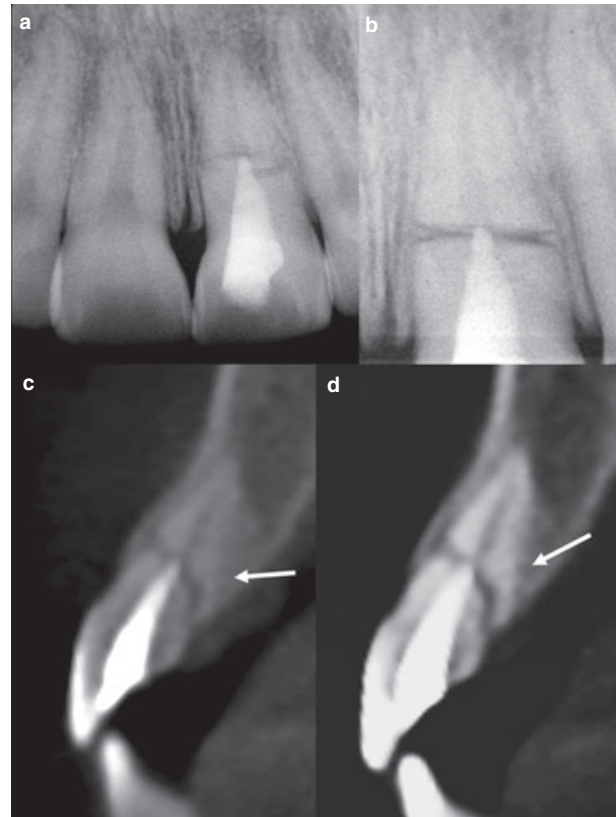


Fig. 4. (a, b) At 10-month follow up the periapical radiograph shows evidence of root remodeling and a significant reduction of the fragments without interposition of granulation tissue. (c, d) NewTom images reveal only a slight reduction in the space between the fragments with interposition of bone and connective tissue. Lack of healing in the palatal surface of the root might be due to a double fracture of the root which can be seen in this cross-sectional proximal view (see arrow).

lucencies were diagnosed and associated with the traumatic displacement of the maxillary left incisors (Fig. 6a–c). A radiopaque particle consistent with a tooth fragment was noted on the soft tissue radiograph of the lower lip (Fig. 6d).

Considering the severity of the trauma, the patient was referred for digital imaging with the NewTom 3G DVT 9000. Images revealed a severe palatal displacement of the maxillary left central incisor with concomitant alveolar fracture and the lack of cortical bone buccal to the maxillary left central and lateral incisors (Fig. 7). The tooth fragment embedded on the lower lip was also detected (Fig. 7b). The emergency treatment protocol included repositioning (Fig. 8) and stabilization of the luxated teeth with acid-etched composite and a flexible wire. The tooth fragment was surgically removed from the lower lip and the patient given amoxycillin 1500 mg daily for a week.

Upon the patient's request he was referred to his general dentist for the endodontic therapy of both



Fig. 5. (a) Preoperative clinical photograph immediately after admission at the emergency room. (b) Intraoral examination showing a severe lateral luxation of both maxillary left incisors and injury of adjacent soft tissue. (c) Occlusal view of the displaced teeth. (d) Soft tissue lacerations and localized swelling of the lower lip is evident.

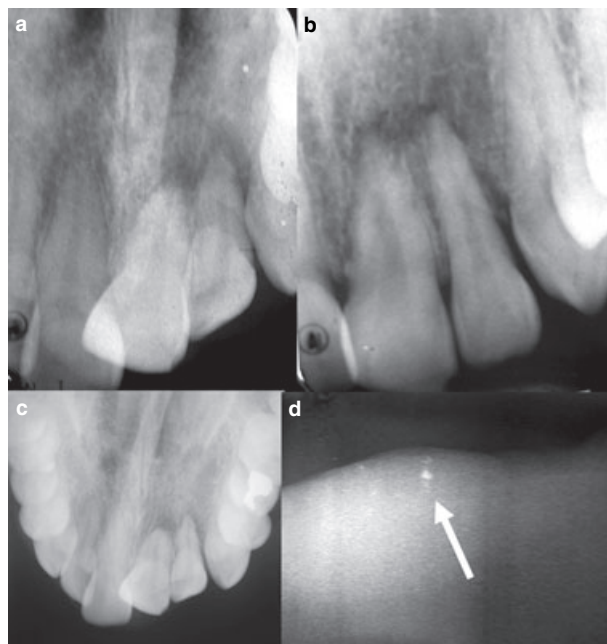


Fig. 6. (a, b) Periapical radiographs demonstrating periradicular radiolucencies associated with the traumatic displacement of the maxillary left incisors. (c) Occlusal radiograph of the pre-maxilla. (d) A radiopaque particle consistent with a tooth fragment is apparent on the soft tissue radiograph of the lower lip.

maxillary left incisors, removal of the splint and follow up of the adjacent teeth. Recall of the patient was not possible due to lack of compliance.

Case 3

A 25-year-old male patient presented to the Center for Urgent Care, Trauma and Sports Dentistry at the University of Southern California 24 hours after

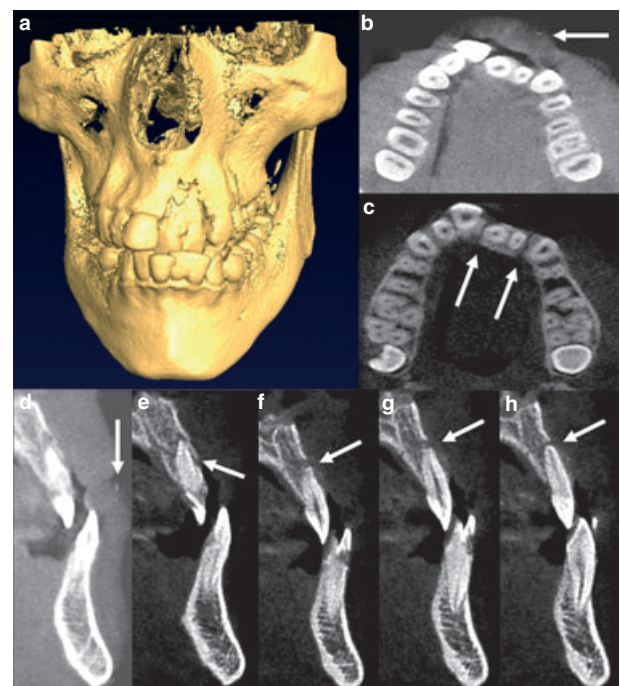


Fig. 7. (a) Frontal reconstruction with the NewTom showing the severity of the impact and subsequent trauma to the left pre-maxilla. (b) The tooth fragment embedded on the lower lip was also detected in this axial view (see arrow). (c) A different axial cut reveals a severe palatal displacement of the maxillary left central incisor and alveolar fracture of the palatal bone. (d–h) Series of cross-sectional 0.2 mm cuts showing lateral luxation of the teeth with concomitant alveolar fracture of the buccal cortical plate (see arrows).

being elbowed during a basketball game. The patient reported that as a result of the injury, his maxillary left central incisor was 'pushed back' and



Fig. 8. Clinical photograph showing repositioning of the maxillary left central and lateral incisors.

he repositioned the tooth by himself. His medical history was noncontributory.

Extraoral examination revealed no significant abnormality. Intraoral examination revealed soft tissue lacerations on the attached gingiva as well as on the upper lip (Fig. 9a). No occlusal interferences were observed. Both maxillary left incisors were tender to percussion and with 1–2 mm mobility. The maxillary left central incisor did not respond to vitality testing, although the adjacent teeth responded within normal limits. Radiographic examination showed a slight displacement of the maxillary left central incisor (Fig. 9b,c). Further examination with the NewTom 3G DVT 9000 disclosed a more severe lateral luxation of the maxillary left central incisor with subsequent alveolar fracture of the buccal cortical bone (Fig. 10a–d). The maxillary

right central incisor was not displaced as a result of the trauma (Fig. 10e). No splint was required as the teeth were stable and the patient was rescheduled for a follow-up examination.

Ten days later the patient presented with marked crown discoloration on the maxillary left central incisor. Clinically, the tooth was asymptomatic and there was no sensitivity to percussion or palpation. Radiographic examination showed no evidence of pathology. Based on the available data, a conservative approach was recommended and the patient followed up clinically and radiographically every 6 weeks. Four months later following a thorough clinical and radiographic examination, the maxillary left central incisor was diagnosed with pulp necrosis. The treatment plan included root canal therapy, intracoronal bleaching and coronal restoration of the maxillary left central incisor and follow up of the adjacent teeth. The treatment was uneventful and the patient remained asymptomatic.

Eleven months later a radiographic examination (Fig. 11) showed evidence of apical bone remodeling and new buccal cortical bone formation apical to the maxillary left central incisor (Fig. 11c).

Discussion

Most maxillofacial traumatic injuries involve the dentition alone (50%), or both the dentition and adjacent soft tissue (36%) (48). Maxillofacial fractures (13.6%) account for the remaining types of injury. Traumatized teeth present a clinical challenge with regard to their diagnosis, treatment plan,

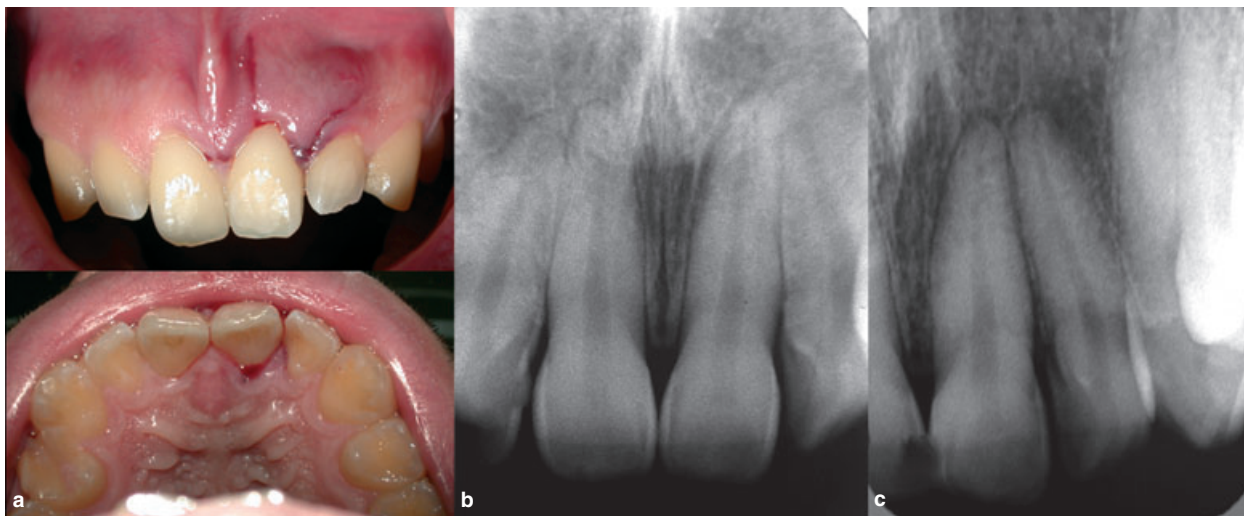


Fig. 9. (a) Soft tissue lacerations on the attached gingiva and the upper lip. (b, c) Radiographs showing slight enlargement of the periodontal ligament space on the mesial and apical aspects of the maxillary left central incisor due to the traumatic displacement of the tooth.

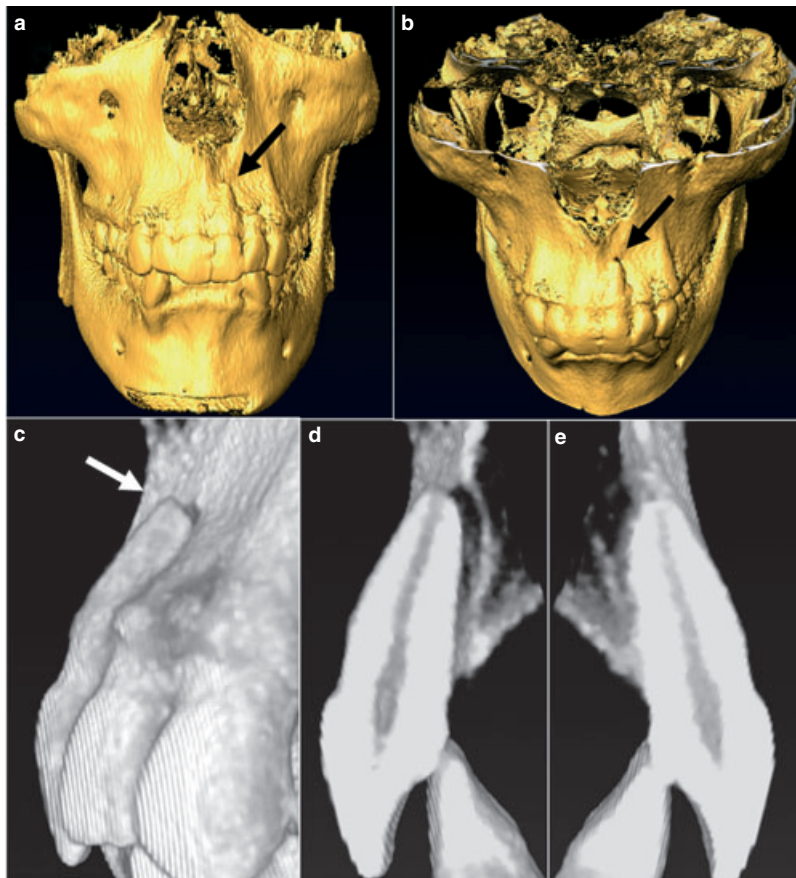


Fig. 10. (a, b) Frontal reconstruction with the NewTom demonstrating luxation of the maxillary left central incisor with concomitant alveolar fracture. (c, d) Cross-sectional views showing lateral luxation of the maxillary left central incisor. (e) No evidence of traumatic displacement is noted on the maxillary right central incisor as result of the trauma.

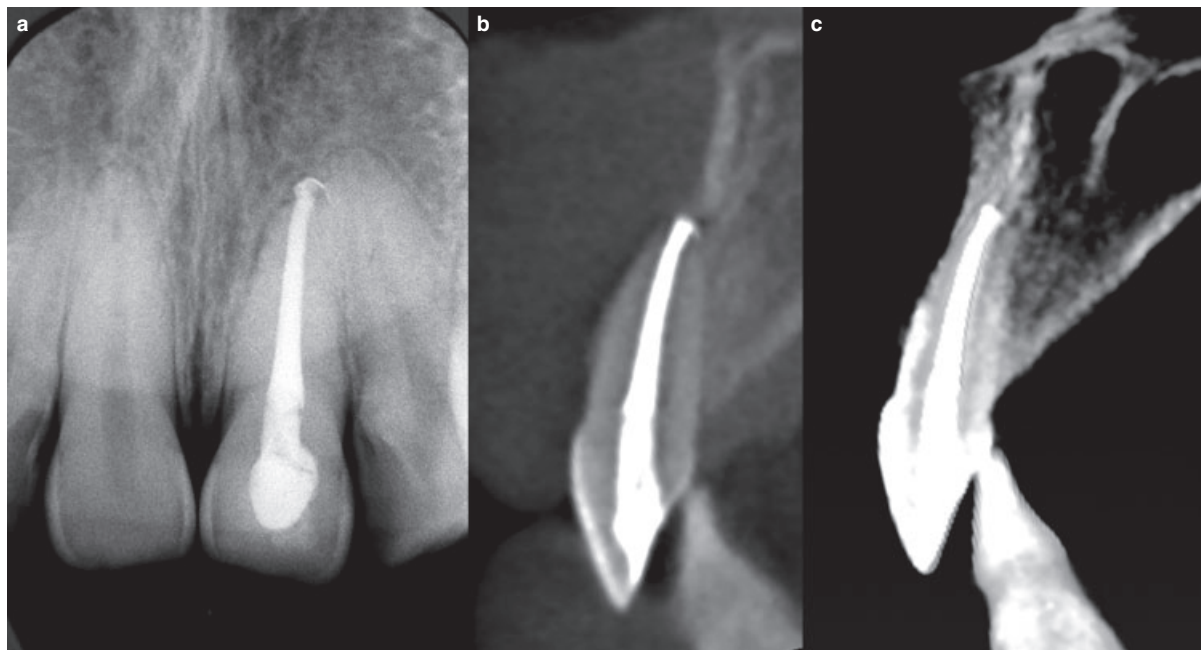


Fig. 11. Eleven-month follow-up. (a) The periapical radiograph shows evidence of apical bone remodeling. (b, c) Cross-sectional images demonstrate periradicular normalcy and new buccal cortical bone formation apical to the maxillary left central incisor.

and prognosis. Unfortunately, film-based intraoral radiography provides poor sensitivity in the detection of minimal tooth displacements, root, and

alveolar fractures (49). This limitation is due to the projection geometry, superimposition of anatomic structures, and processing errors.

The application of computer-based systems and the development of electronic sensors have provided the technical means to apply theoretical principles to diagnostic imaging. Among these innovations, CBCT has significantly improved the ability to accurately diagnose traumatic injuries with the potential to overcome most of the technical limitations of the plain film projection and the capability of providing a 3-D representation of the maxillofacial tissues in a cost- and dose-efficient manner (50). However, at present, traditional radiographs will not be replaced by CBCT as the image resolution for 3-D imaging is still inferior to radiograph image resolution and the equipment is still quite expensive.

In our study subjects, the NewTom 3G DVT 9000 provided valuable information that helped us to determine the type and severity of the injury. Subsequently, we were able to establish the appropriate treatment plan and its implementation. The examples illustrated in this paper highlight the need for treatment planning based on a comprehensive evaluation by all diagnostic modalities available including new digital imaging techniques.

References

1. Akdeniz BG, Sogur E. An ex vivo comparison of conventional and digital radiography for perceived image quality of root fillings. *Int Endod J* 2005;38:397–401.
2. Nair MK, Nair UDP, Grondahl HG, Webber RL, Wallace JA. Detection of artificially induced vertical radicular fractures using tuned aperture computed tomography. *Eur J Oral Sci* 2001;109:375–9.
3. Tanrikulu R, Erol B. Comparison of computed tomography with conventional radiography for midfacial fractures. *Dentomaxillofac Radiol* 2001;30:141–6.
4. Abreu M Jr, Yi-Ching L, Abreu AL. Comparative diagnostic performance of TACT slices and its multiple source images: an in vitro study. *Dentomaxillofac Radiol* 2004;33:93–7.
5. Klenk G, Kovacs A. Do we need three-dimensional computed tomography in maxillofacial surgery? *J Craniofac Surg* 2004;15:842–50; discussion 850.
6. Ludlow JB, Davies-Ludlow LE, Brooks SL. Dosimetry of two extraoral direct digital imaging devices: NewTom cone beam CT and Orthophos Plus DS panoramic unit. *Dentomaxillofac Radiol* 2003;32:229–34.
7. Danforth RA, Dus I, Mah J. 3-D volume imaging for dentistry: a new dimension. *J Calif Dent Assoc* 2003;31:817–23.
8. Marmulla R, Wortche R, Muhling J, Hassfeld S. Geometric accuracy of the NewTom 9000 Cone Beam CT. *Dentomaxillofac Radiol* 2005;34:28–31.
9. Mozzo P, Procacci C, Tacconi A, Martini PT, Andreis IA. A new volumetric CT machine for dental imaging based on the cone-beam technique: preliminary results. *Eur Radiol* 1998;8:1558–64.
10. Trope M, Pettigrew J, Petras J, Barnett F, Tronstad L. Differentiation of radicular cyst and granulomas using computerized tomography. *Endod Dent Traumatol* 1989;5:69–72.
11. Shrout MK, Hall JM, Hildebolt CE. Differentiation of periapical granulomas and radicular cysts by digital radiometric analysis. *Oral Surg Oral Med Oral Pathol* 1993;76:356–61.
12. Cotti E, Vargiu P, Dettori C, Mallarini G. Computerized tomography in the management and follow-up of extensive periapical lesion. *Endod Dent Traumatol* 1999;15:186–9.
13. Camps J, Pommel L, Bukiet F. Evaluation of periapical lesion healing by correction of gray values. *J Endod* 2004;30:762–6.
14. Ziegler CM, Woertche R, Brief J, Hassfeld S. Clinical indications for digital volume tomography in oral and maxillofacial surgery. *Dentomaxillofac Radiol* 2002;31:126–30.
15. Mah J, Enciso R, Jorgensen M. Management of impacted cuspids using 3-D volumetric imaging. *J Calif Dent Assoc* 2003;31:835–41.
16. Alder ME, Deahl ST, Matteson SR. Clinical usefulness of two-dimensional reformatted and three-dimensionally rendered computerized tomographic images: literature review and a survey of surgeons' opinions. *J Oral Maxillofac Surg* 1995;53:375–86.
17. Blinkhorn FA. The aetiology of dento-alveolar injuries and factors influencing attendance for emergency care of adolescents in the north west of England. *Endod Dent Traumatol* 2000;16:162–5.
18. Sgan-Cohen HD, Megnagi G, Jacobi Y. Dental trauma and its association with anatomic, behavioral, and social variables among fifth and sixth grade schoolchildren in Jerusalem. *Community Dent Oral Epidemiol* 2005;33:174–80.
19. Andreasen JO, Andreasen FM. Classification, etiology and epidemiology. In: Andreasen F, editor. *Textbook and color atlas of traumatic injuries to the teeth*, 3rd edn. Copenhagen: Munksgaard; 1994. pp 151–77.
20. Andreasen FM. Histological and bacteriological study of pulps extirpated after luxation injuries. *Endod Dent Traumatol* 1988;4:170–81.
21. Matteson SR, Deahl ST, Alder ME, Nummikoski PV. Advanced imaging methods. *Crit Rev Oral Biol Med* 1996;7:346–95.
22. Fullerton GD, Potter JL. Computed tomography. In: Putman CE, Ravin CE, editors. *Textbook of diagnostic imaging*. Philadelphia: W.B. Saunders; 1988. pp 47–61.
23. Hounsfield GN. Computerized transverse axial scanning (tomography). 1. Description of system. *Br J Radiol* 1973;46:1016–22.
24. Kalra MK, Maher MM, D'Souza R, Saini S. Multidetector computed tomography technology: current status and emerging developments. *J Comput Assist Tomogr* 2004;28(Suppl. 1):S2–6.
25. Flohr TG, Schaller S, Stierstorfer K, Bruder H, Ohnesorge BM, Schoepf UJ. Multi-detector row CT systems and image-reconstruction techniques. *Radiology* 2005;235:756–73.
26. Finkle DR, Ringler SL, Luttenton CR, Beernink JH, Peterson NT, Dean RE. Comparison of the diagnostic methods used in maxillofacial trauma. *Plast Reconstr Surg* 1985;75:32–41.
27. Hornak JP. The basics of MRI. <http://www.cis.rit.edu/htbooks/mri/>; 2003.
28. Damadian R, Goldsmith M, Minkoff L. NMR in cancer: XVI. FONAR image of the live human body. *Physiol Chem Phys* 1977;9:97–100, 108.
29. Mansfield P, Maudsley AA. Medical imaging by NMR. *Br J Radiol* 1977;50:188–94.
30. Fukatsu H. 3T MR for clinical use: update. *Magn Reson Med Sci* 2003;2:37–45.
31. Laine FJ, Conway WF, Laskin DM. Radiology of maxillofacial trauma. *Curr Probl Diagn Radiol* 1993;22:145–88.
32. Danforth RA, Peck J, Hall P. Cone beam volume tomography: an imaging option for diagnosis of complex

- mandibular third molar anatomical relationships. *J Calif Dent Assoc* 2003;31:847–52.
33. Eggers G, Mukhamadiev D, Hassfeld S. Detection of foreign bodies of the head with digital volume tomography. *Dentomaxillofac Radiol* 2005;34:74–9.
 34. Sato S, Arai Y, Shinoda K, Ito K. Clinical application of a new cone-beam computerized tomography system to assess multiple two-dimensional images for the preoperative treatment planning of maxillary implants: case reports. *Quintessence Int* 2004;35:525–8.
 35. Hatcher DC, Dial C, Mayorga C. Cone beam CT for pre-surgical assessment of implant sites. *J Calif Dent Assoc* 2003;31:825–33.
 36. Baumrind S, Carlson S, Beers A, Curry S, Norris K, Boyd RL. Using three-dimensional imaging to assess treatment outcomes in orthodontics: a progress report from the University of the Pacific. *Orthod Craniofac Res* 2003;6(Suppl. 1):132–42.
 37. Maki K, Inou N, Takanishi A, Miller AJ. Computer-assisted simulations in orthodontic diagnosis and the application of a new cone beam X-ray computed tomography. *Orthod Craniofac Res* 2003;6(Suppl. 1):95–101; discussion 179–82.
 38. Hilgers ML, Scarfe WC, Scheetz JP, Farman AG. Accuracy of linear temporomandibular joint measurements with cone beam computed tomography and digital cephalometric radiography. *Am J Orthod Dentofacial Orthop* 2005;128:803–11.
 39. Lascalea CA, Panella J, Marques MM. Analysis of the accuracy of linear measurements obtained by cone beam computed tomography (CBCT-NewTom). *Dentomaxillofac Radiol* 2004;33:291–4.
 40. Ngan DC, Kharbanda OP, Geenty JP, Darendeliler MA. Comparison of radiation levels from computed tomography and conventional dental radiographs. *Aust Orthod J* 2003;19:67–75.
 41. Danforth RA, Clark DE. Effective dose from radiation absorbed during a panoramic examination with a new generation machine. *Oral Surg Oral Med Oral Pathol Oral Radiol Endod* 2000;89:236–43.
 42. Gibbs SJ. Effective dose equivalent and effective dose: comparison for common projections in oral and maxillofacial radiology. *Oral Surg Oral Med Oral Pathol Oral Radiol Endod* 2000;90:538–45.
 43. Hashimoto K, Arai Y, Iwai K, Araki M, Kawashima S, Terakado M. A comparison of a new limited cone beam computed tomography machine for dental use with a multidetector row helical CT machine. *Oral Surg Oral Med Oral Pathol Oral Radiol Endod* 2003;95:371–7.
 44. Mah JK, Danforth RA, Bumann A, Hatcher D. Radiation absorbed in maxillofacial imaging with a new dental computed tomography device. *Oral Surg Oral Med Oral Pathol Oral Radiol Endod* 2003;96:508–13.
 45. Imamura H, Sato H, Matsuura T, Ishikawa M, Zeze R. A comparative study of computed tomography and magnetic resonance imaging for the detection of mandibular canals and cross-sectional areas in diagnosis prior to dental implant treatment. *Clin Implant Dent Relat Res* 2004;6:75–81.
 46. Nasel CJ, Pretterklieber M, Gahleitner A, Czerny C, Breitenseher M, Imhof H. Osteometry of the mandible performed using dental MR imaging. *AJNR Am J Neuroradiol* 1999;20:1221–7.
 47. Gahleitner A, Solar P, Nasel C, Homolka P, Youssefzadeh S, Ertl L et al. Magnetic resonance tomography in dental radiology (dental MRI). *Radiologe* 1999;39:1044–50.
 48. Gassner R, Bosch R, Tuli T, Emshoff R. Prevalence of dental trauma in 6000 patients with facial injuries: implications for prevention. *Oral Surg Oral Med Oral Pathol Oral Radiol Endod* 1999;87:27–33.
 49. Kositbowornchai S, Nuansakul R, Sikram S, Sinahawatana S, Saengmontri S. Root fracture detection: a comparison of direct digital radiography with conventional radiography. *Dentomaxillofac Radiol* 2001;30:106–9.
 50. Scarfe WC. Imaging of maxillofacial trauma: evolutions and emerging revolutions. *Oral Surg Oral Med Oral Pathol Oral Radiol Endod* 2005;100(Suppl. 2):S75–96.

This document is a scanned copy of a printed document. No warranty is given about the accuracy of the copy. Users should refer to the original published version of the material.